Eur. J. Mech. B - Fluids 20 (2001) 75–86

S0997-7546(00)01099-2/FLA

Nonlinear investigation of anti-convection and Rayleigh–Benard convection in systems with heat release at the interface

Alexander A. Nepomnyashchy [a,b], Ilya B. Simanovskii [a,*]

[a] *Department of Mathematics, Technion, Israel Institute of Technology, 32000 Haifa, Israel*
[b] *Minerva Center for Nonlinear Physics of Complex Systems, Technion, Israel Institute of Technology, 32000 Haifa, Israel*

(Received 1 December 1999; revised 15 May 2000; accepted 31 May 2000)

Abstract – Anti-convection and Rayleigh–Benard convection generated by the joint action of external heating and heat sources (sinks) on the interface in layers with finite thicknesses are studied. Numerical simulations of the finite-amplitude convective regimes have been mage for the real two-liquid system (silicone oil 10 cs – ethylenglycol), convenient for the performance of experiments. The nonlinear boundary value problem was solved by means of the finite-difference method. Anti-convective structures in fluid systems subject to anti-convective instability only in the presence of heat sources (sinks) on the interface, have been obtained. This new type of the anti-convective motion appears in the case where one layer is strongly heated from above, while the temperature gradient in another layer is very weak. © 2001 Éditions scientifiques et médicales Elsevier SAS

1. Introduction

It can be found in any textbooks that, for fluids with positive heat expansion coefficient, the buoyancy convective instability of equilibrium appears only by heating from below [1]. Paradoxically, this is not actually correct in the presence of an interface between two fluids. It was shown by Welander [2], that thermal and hydrodynamic phenomena on the interface may lead to a buoyancy convective instability by heating from above ('anti-convection'). The anti-convective mechanism of instability appears only under specific conditions: fluids with considerably different physical properties must be considered. Particularly, the heat expansion coefficient of the upper fluid must be much smaller than the heat expansion coefficient of the lower fluid and the thermal diffusivity of the lower fluid must be much higher than the thermal diffusivity of the upper one, or vice versa [2–4].

For a long time it was a common opinion that the phenomenon of anti-convection was rather exotic and that, as the matter of fact, only one physical system (water-mercury), satisfied the conditions for the existence of anti-convection had been found [3]. It turns out, however, that anti-convection can appear also in the presence of a uniformly distributed heat source (sink) at the interface. In this case, the anti-convective and buoyancy instability mechanisms can act simultaneously. The interaction between both instability mechanisms for the water-mercury system was studied in [5]. In [6] it was found that, in the presence of an interfacial heat source (sink), the anti-convection could be generated in any system of two semi-infinite layers. The general analysis of the conditions for the appearance of anti-convection in a system of layers with finite thicknesses was performed in [7]. It was shown that anti-convection appears in the situation where the temperature gradient in one fluid is much smaller than that in the other fluid. The difference between the temperature gradients sufficient for the appearance of anti-convection, can be caused by the natural difference of thermophysical parameters of the

* Correspondence and reprints.
E-mail address: mathsec@tx.technion.ac.il (I.B. Simanovskii).

fluids, as in the case of the water-mercury system, or it can be produced artificially by heating or cooling the interface.

Let us describe the physical mechanism of anti-convection in a system of two fluids heated from above in the case where the temperature gradient in the upper layer is large in comparison with that in the lower layer. Consider a positive temperature fluctuation at a certain point at the interface. This fluctuation generates an ascending convective flow in the lower fluid under this point. Because the vertical temperature gradient in the lower fluid is small, the heat transfer caused by this flow is not sufficient to neutralize the initial positive temperature fluctuation. The motion generated in the upper fluid is caused by two competing factors: the temperature fluctuation tends to produce an ascending flow, while the viscous stresses on the interface tend to produce a descending flow. Near the interface, the viscous coupling prevails; thus there appears a descending flow that supplies a hot fluid to the interface. If the positive temperature gradient in the upper fluid is strong enough, the initial positive temperature fluctuation is enhanced, and the anti-convection develops in the system. The appearance of anti-convection in the opposite case where the vertical temperature gradient is relatively small in the upper fluid and large in the lower fluid, can be explained in a similar way.

In the present paper the numerical investigation of the combined action of anti-convection and Rayleigh–Benard convection in a system with a heat release at the interface is investigated.

In section 2, the mathematical formulation of the problem and numerical method are presented. Sections 3 and 4 are devoted to the consideration of anti-convection and Rayleigh–Benard convection generated by the joint action of the external heating and heat release on the interface. Section 5 contains some concluding remarks.

2. Formulation of the problem and numerical method

Let a rectangular cavity with rigid boundaries be filled by two immiscible viscous fluids (see *figure 1*). The plates are kept at different constant temperatures (the total temperature drop is θ). Two different variants of external heating, from above and from below, are considered. Let a constant heat release of rate Q_0 (Q_0 may be positive or negative) be set on the interface. Deformation of the interface is not taken into account. All variables

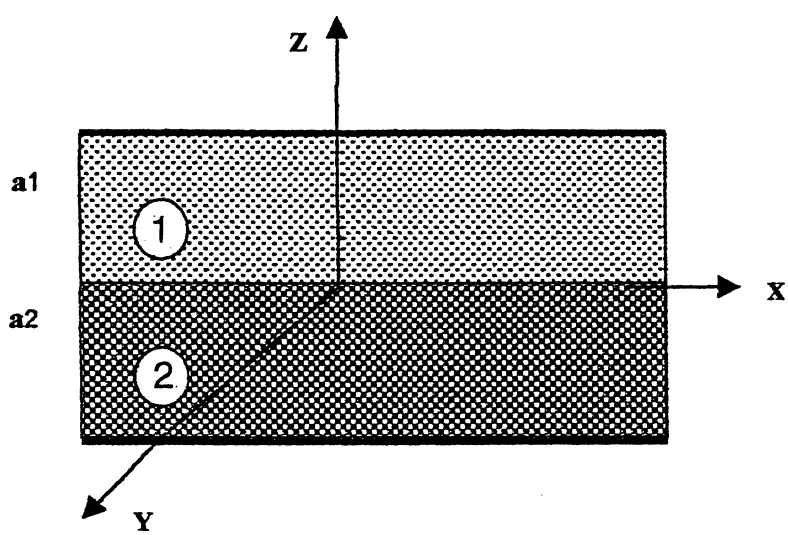

Figure 1. Geometrical configuration of the two-layer system and coordinate axes.

referring to the upper layer are indicated by index 1, and the variables referring to the lower layer by index 2. Densities, coefficients of dynamic and kinematic viscocities, heat conductivities, thermal diffusivities and heat expansion coefficients of the mth fluid are equal to $\rho_m, \eta_m, \nu_m, \kappa_m, \chi_m, \beta_m$ $(m = 1, 2)$, respectively.

The mechanical equilibrium state is characterized by constant values of vertical temperature gradients A_m $(m = 1, 2)$, which are found from the heat balance condition on the interface $-\kappa_1 A_1 + \kappa_2 A_2 = Q_0$ and the relation $A_1 a_1 + A_2 a_2 = -s\theta$ ($s = 1$ when heating is from below and $s = -1$ when heating is from above):

$$A_1 = -(s\theta\kappa_2 + Q_0 a_2)/(a_1\kappa_2 + a_2\kappa_1),$$
$$A_2 = -(s\theta\kappa_1 - Q_0 a_1)/(a_1\kappa_2 + a_2\kappa_1).$$

The notation $\rho = \rho_1/\rho_2,\ \eta = \eta_1/\eta_2\ \nu = \nu_1/\nu_2,\ \kappa = \kappa_1/\kappa_2,\ \chi = \chi_1/\chi_2,\ \beta = \beta_1/\beta_2,\ a = a_2/a_1$ is introduced. As the units of length, time, velocity, pressure and temperature we use $a_1,\ a_1^2/\nu_1,\ \nu_1/a_1,\ \rho_1\nu_1^2/a_1^2$ and θ, respectively. Dimensionless temperature gradients in the equilibrium state are:

$$A_1 = -\frac{sG + a\kappa G_Q}{G(1+\kappa a)}, \qquad A_2 = -\frac{\kappa(sG - G_Q)}{G(1+\kappa a)}; \tag{1}$$
$$G = \frac{g\beta_1\theta a_1^3}{\nu_1^2}; \qquad G_Q = \frac{g\beta_1 Q_0 a_1^4}{\nu_1^2\kappa_1}.$$

Here G is the Grashof number characterising the intensity of the external heating (g is the acceleration due to gravity), and G_Q is the modified Grashof number determined by the intensity of the interfacial heat release.

Note that for each layer we can define its own ('local') Rayleigh number:

$$R_m = -\frac{g\beta_m \tilde{A}_m a_m^4}{\nu_m \chi_m}, \quad m = 1, 2,$$

where $\tilde{A}_m$ is a dimensional temperature gradient in the mth fluid (the Rayleigh number is assumed to be positive (negative) if the corresponding temperature gradient is negative (positive)). Values of R_m are not independent. They are expressed via dimensionless parameters defined above, in the following way:

$$R_1 = \frac{(sG + a\kappa G_Q)P}{G(1+\kappa a)}, \qquad R_2 = \frac{\kappa(sG - G_Q)}{G(1+\kappa a)} \cdot \frac{\nu\chi a^4}{\beta}.$$

The complete nonlinear equations of convection in the framework of the Boussinesq approximation (see [8]) for both fluids have the following form:

$$\frac{\partial v_m}{\partial t} + (\vec{v}_m\nabla)\vec{v}_m = -\nabla p_m + c_m\nabla^2\vec{v}_m + Gb_m T_m\vec{\gamma},$$
$$\frac{\partial T_m}{\partial t} + \vec{v}_m\nabla T_m = \frac{d_m}{P}\nabla^2 T_m, \tag{2}$$
$$\nabla\vec{v}_m = 0 \quad (m = 1, 2).$$

Here $b_1 = c_1 = d_1 = 1,\ b_2 = 1/\beta,\ c_2 = 1/\nu,\ d_2 = 1/\chi$, and $P = \nu_1/\chi_1$ is the Prandtl number, $\vec{\gamma}$ is the unit vector directed vertically upward. The conditions on the isothermic rigid horizontal boundaries are:

$$z = 1: \ \vec{v}_1 = 0;\ T_1 = 0,$$
$$z = -a: \ \vec{v}_2 = 0;\ T_2 = s, \tag{3}$$

$s = 1$ for heating from below, $s = -1$ for heating from above.

The boundary conditions on the interface $z = 0$ include conditions for the tangential stresses:

$$z = 0\text{: } \eta\frac{\partial v_{1x}}{\partial z} = \frac{\partial v_{2x}}{\partial z},\ \eta\frac{\partial v_{1y}}{\partial z} = \frac{\partial v_{2y}}{\partial z}; \tag{4}$$

the continuity of the velocity field:

$$z = 0\text{: } \vec{v}_1 = \vec{v}_2; \tag{5}$$

the continuity of the temperature field:

$$z = 0\text{: } T_1 = T_2; \tag{6}$$

and the continuity of the heat flux normal components

$$z = 0\text{: } \kappa\frac{\partial T_1}{\partial z} = \frac{\partial T_2}{\partial z} - \kappa\frac{G_Q}{G}. \tag{7}$$

The conditions on the solid lateral boundaries, which are assumed thermally insulated, are:

$$x = -\frac{L}{2}, \frac{L}{2}\text{: } \vec{v}_m = 0;\ \frac{\partial T_m}{\partial x} = 0; \quad m = 1, 2. \tag{8}$$

We have performed nonlinear simulations of two-dimensional flows ($v_{my} = 0$; the fields of physical variables do not depend on y). In this case, we can introduce the stream function

$$v_{mx} = \frac{\partial \psi_m}{\partial z}, \qquad v_{mz} = -\frac{\partial \psi_m}{\partial x} \quad (m = 1, 2).$$

Eliminating the pressure and defining the vorticity

$$\varphi_m = \frac{\partial v_{mz}}{\partial x} - \frac{\partial v_{mx}}{\partial z},$$

we can rewrite the boundary value problem, equations (2)–(8), in the following form:

$$\frac{\partial \varphi_m}{\partial t} + \frac{\partial \psi_m}{\partial z}\frac{\partial \varphi_m}{\partial x} - \frac{\partial \psi_m}{\partial x}\frac{\partial \varphi_m}{\partial z} = c_m\Delta\varphi_m + Gb_m\frac{\partial T_m}{\partial x}, \tag{9}$$

$$\frac{\partial T_m}{\partial t} + \frac{\partial \psi_m}{\partial z}\frac{\partial T_m}{\partial x} - \frac{\partial \psi_m}{\partial x}\frac{\partial T_m}{\partial z} = \frac{d_m}{P}\nabla^2 T_m, \tag{10}$$

$$\nabla^2\psi_m = -\varphi_m, \quad m = 1, 2, \tag{11}$$

$$z = 1\text{: } \psi_1 = \frac{\partial \psi_1}{\partial z} = 0;\ T_1 = 0; \tag{12}$$

$$z = -a\text{: } \psi_2 = \frac{\partial \psi_2}{\partial z} = 0;\ T_2 = s; \tag{13}$$

$$z = 0\text{: } \psi_1 = \psi_2 = 0,\ \frac{\partial \psi_1}{\partial z} = \frac{\partial \psi_2}{\partial z}, \tag{14}$$

$$T_1 = T_2,\ \kappa\frac{\partial T_1}{\partial z} = \frac{\partial T_2}{\partial z} - \kappa\frac{G_Q}{G}; \tag{15}$$

$$x = -\frac{L}{2}, \frac{L}{2}\text{: } \psi_m = \frac{\partial \psi_m}{\partial x} = \frac{\partial T_m}{\partial x} = 0; \quad m = 1, 2. \tag{16}$$

The boundary value problem equations (9)–(16) was solved by the finite-difference method. Equations and boundary conditions were approximated on a uniform mesh using a second order approximation for the spatial coordinates. The nonlinear equations were solved using an explicit scheme on a rectangular uniform 56×56 mesh. The time step was calculated by the formula

$$\Delta t = \frac{[\min(\Delta x, \Delta z)]^2[\min(1, \nu, \chi)]}{2[2 + \max|\psi_m(x, z)|]} \quad (m = 1, 2).$$

The Poisson equation was solved by the iterative Liebman successive over-relaxation method on each time step: the accuracy of the solution was 10^{-4}. The Kuskova and Chudov formulas [9], providing the second order accuracy, were used for the approximation of the vorticity on the on the solid boundaries.

At the interface the expression for the vorticity is approximated with the second-order accuracy for the spatial coordinates and have a form:

$$\varphi_1(x, 0) = -\frac{2[\psi_2(x, -\Delta z) + \psi_1(x, \Delta z)]}{(\Delta z)^2(1 + \eta)}, \tag{17}$$

$$\varphi_2(x, 0) = \eta\varphi_1(x, 0). \tag{18}$$

Here Δx, Δz are the mesh sizes for the corresponding coordinates. The temperatures on the interfaces were calculated by the second-order approximation formulas:

$$T_1(x, 0) = T_2(x, 0) = \frac{[4T_2(x, -\Delta z) - T_2(x, -2\Delta z)] + \kappa[4T_1(x, \Delta z) - T_1(x, 2\Delta z)]}{3(1 + \kappa)}. \tag{19}$$

The details of the scheme may be found in [8].

3. Anti-convection

In this section we present the results of the numerical solution of the boundary-value problem equations (9)–(16) for the real two-liquid system silicone oil 10 cs – ethylenglycol with the following set of parameters: $\rho = 0.846$, $\eta = 0.549$, $\nu = 0.6493$, $\kappa = 0.6194$, $\chi = 1.096$, $\beta = 1.4516$; the Prandtl number $P = 94$. The calculations were made with $L = 4$, $a = 1$. The above-mentioned pair of fluids is convenient for the performance of experiments [10]. The interfacial heating may be generated, e.g. by an infrared light source. The infrared absorption bands of alcohols and silicone fluids are rather different [11] therefore the light frequency can be chosen in such a way that one of the fluids is transparent, while the characteristic length of the light absorption in another fluid is short.

Let us emphasize that in the absence of the heat release on the interface the anti-convection in this system is impossible. However, as explained in section 1, one can expect the appearance of anti-convection in two cases: (i) $0 < A_1 \ll A_2$; (ii) $0 < A_2 \ll A_1$. According to equation (1), the first case takes place as $G_Q > 0$, $sG < -a\kappa G_Q$ ($s = -1$, heating from above) and sG is close to $-a\kappa G_Q$. Similarly, the second case takes place as $s = -1$, $sG < G_Q < 0$, and sG is close to G_Q.

Let us describe briefly the predictions of the linear stability theory for the system of fluids which fill infinite layers with equal thicknesses [7]. The neutral curve, corresponding to the case of heat sources, is shown in *figure 2* (line 1). In the minimum of this neutral curve $sG \approx -3729$ is less than $-a\kappa G_Q \approx -3718$, thus both gradients A_1 and A_2 are positive (see (1)), and the anti-convection is the only instability mechanism. In the point of minimum the ratio $A_1/A_2 \approx 2.4 \cdot 10^{-3}$, i.e. there is a strong heating from above in the lower layer, and nearly

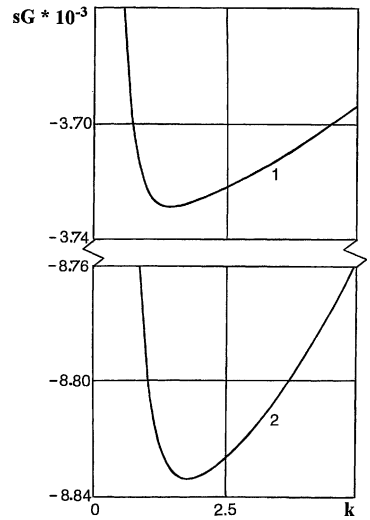

Figure 2. Neutral curves for the anti-convection at $G_Q = 6000$ (line 1) and $G_Q = -8835$ (line 2).

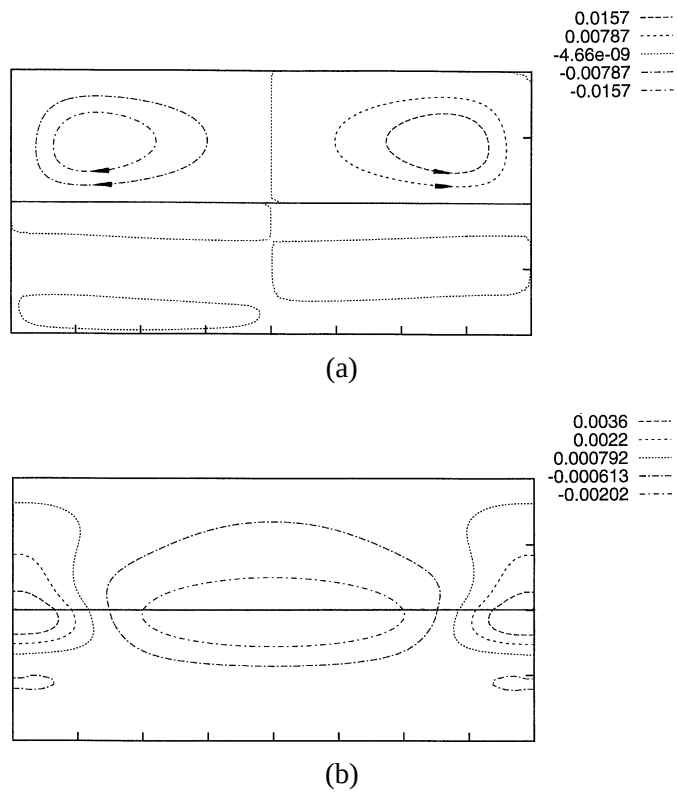

Figure 3. Streamlines (a) and isolines of the temperature deviations (b) for $G = 3717$, $G_Q = 6000$.

neutral stratification in the upper layer. Line 2 in *figure 2* corresponds to the opposite case $G_Q < 0$, $sG \approx G_Q$, characterized by nearly vanishing temperature gradient in the lower layer, and strong positive gradient in the upper layer.

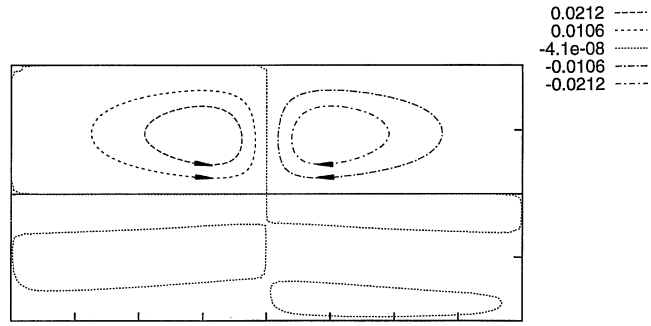

(a)

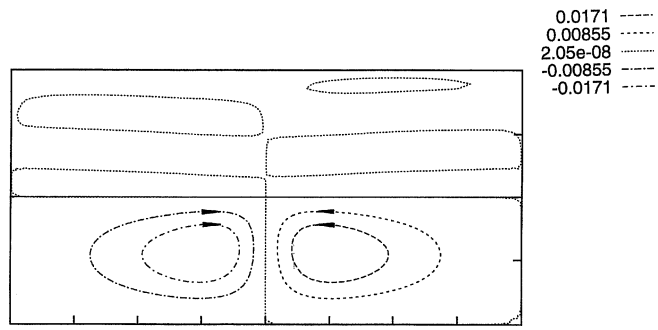

(b)

Figure 4. Streamlines for the steady anti-convective motions: (a) $G = 3717$; $G_Q = 6000$; (b) $G = 15000$.

Nonlinear results confirm the existence of anti-convection in the system with intensive heat sources ($G_Q > 0$) and intensive heat sinks ($G_Q < 0$). A typical anti-convective flow in the case $G_Q > 0$, $sG < -a\kappa G_Q$ ($0 < A_1 \ll A_2$) is shown in *figure 3*. The stream line patterns are shown in *figure 3*(*a*), while *figure 3*(*b*) presents the fields of temperature deviations

$$T_m(x, z) - T_m^{(0)}(z),$$

where $T_m^{(0)}(z)$ is the equilibrium temperature field corresponding to (1).

In the middle of the cavity, there exists a negative deviation of the temperature (*figure 3*(*b*)) that produces an extensive descending motion in the upper layer (with nearly vanishing temperature gradient), and a relatively weak viscosity-induced ascending motion in the lower layer (with the strong positive gradient) near the interface (*figure 3*(*a*)). However, because of the difference between the temperature gradients in both fluids, the heat transfer to the boundary caused by both motions is balanced, so that a stationary anti-convective flow takes place. Near the lateral boundaries, a positive deviation of the temperature generates an ascending motion in the upper layer and a descending motion near the interface in the lower layer, in a similar way. Note that thermal and viscous coupling between two layers generates a multi-store flow structure in the lower layer. Let us note that at the same values of G and G_Q another type of the anti-convective motion is possible which is characterized by a positive deviation of the temperature in the middle of the cavity and a negative deviation of the temperature near the lateral boundaries. The stream function fields in this case are shown in *figure 4*(*a*). In the opposite case $sG < G_Q < 0$ ($0 < A_2 \ll A_1$) the most intensive motion is realized in the lower layer and the weak induced motion with a multi-store structure appears in the upper layer (see *figure 4*(*b*)). With the decrease in the Grashof number ($G_Q > 0$, $sG > -a\kappa G_Q$ or $G_Q < 0$, $sG > G_Q$), the signs of the equilibrium temperature gradients

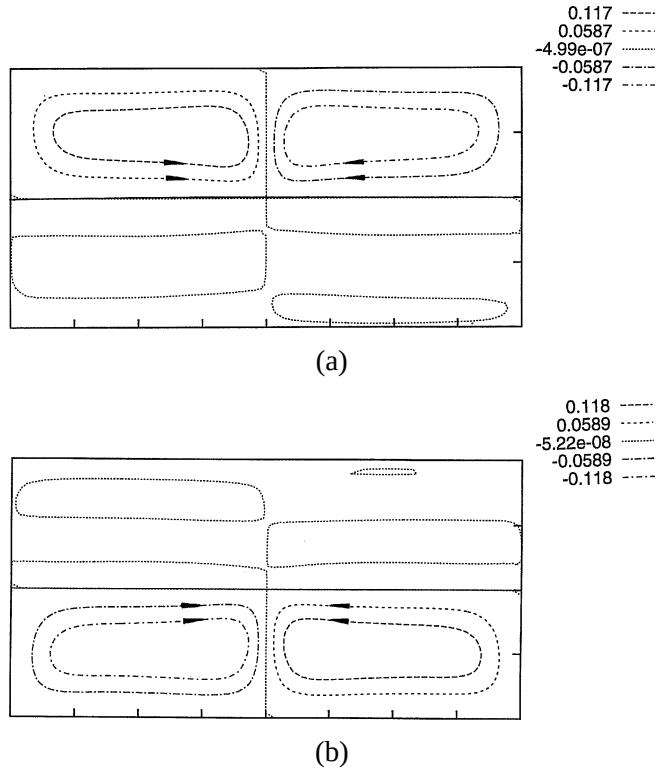

Figure 5. Streamlines in the region of the combined action of anti-convection and Rayleigh–Benard convection: (a) $G = 3000$; $G_Q = 6000$; (b) $G = 11500$; $G_Q = -15000$.

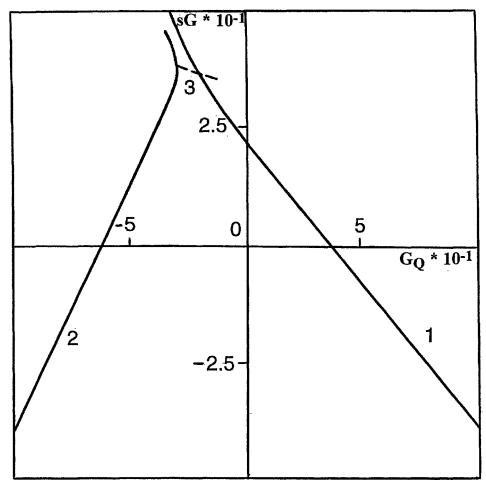

Figure 6. Boundaries of the stability region of the mechanical equilibrium with the respect to monotonic modes (lines 1, 2) and oscillatory mode (line 3).

A_1 and A_2 become different. In this case the anti-convection and the Rayleigh–Benard instability mechanism act simultaneously (see *figure 5*). The influence of the Rayleigh–Benard (bulk) instability mechanism leads to an obvious change of the rolls shape in comparison with that of the pure anti-convection which is essentially connected with the interface (cf. *figure 4*).

4. Rayleigh–Benard convection

The main results of the linear stability theory for the Rayleigh–Benard convection in the abovementioned fluid system are presented in *figure 6*. Line 1 corresponds to the instability caused by negative A_1, while line 2 corresponds to the instability caused by negative A_2. In the region $G_Q < 0$, $sG > 0$ both lines approach each other, and an oscillatory instability (dashed line 3 in *figure 6*) appears, due to the interaction of both monotonic modes.

On the monotonic instability lines 1 and 2, correspondingly, two different types of stationary convective motions appear (type I and type II). Both types of motion obtained in nonlinear simulations with $L = 4$ have the following symmetry property:

$$\psi_m(x, z) = -\psi_m(L - x, z), \qquad T_m(x, z) = T_m(L - x, z); \quad m = 1, 2. \tag{20}$$

The streamline patterns and isotherms corresponding to type I are shown in *figure 7*. One can see that the intensity of motion in the upper layer (where the heating is from below) is larger than the intensity of motion in the lower layer (where the heating is from above). Because of the viscous coupling on the interface, which prevails the thermal coupling between layers, the vortices form a 'chess-order' structure. The structure of motion and isotherms corresponding to type II are presented in *figure 8*. The motion in the lower layer is more intensive than in the upper one. Note that in the latter case the corresponding vortices in lower and upper layers rotate in the same direction, because the thermal coupling prevails. The viscous coupling generates only two weak additional vortices in the upper layer near the interface.

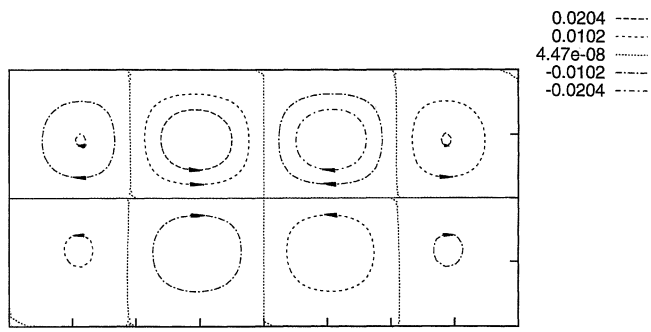

(a)

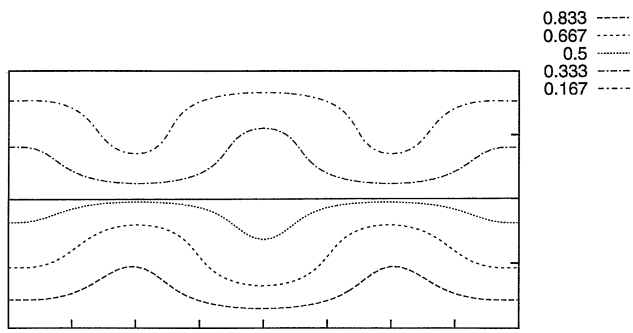

(b)

Figure 7. Streamlines for the Rayleigh–Benard convection: $G = 50$; $G_Q = -25$.

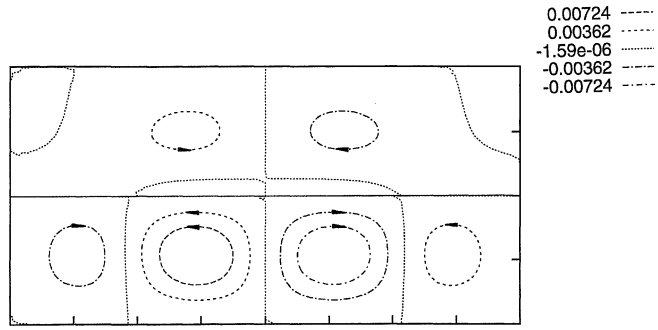

(a)

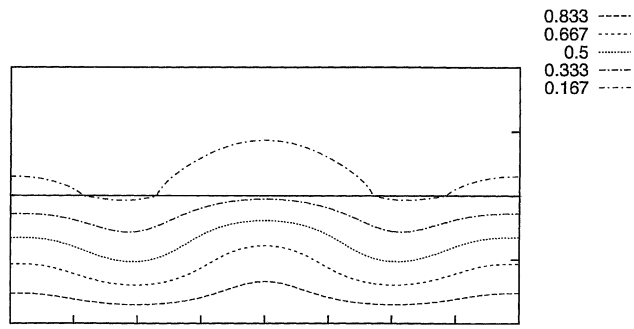

(b)

Figure 8. Streamlines for the Rayleigh–Benard convection: $G = 38$; $G_Q = -45$.

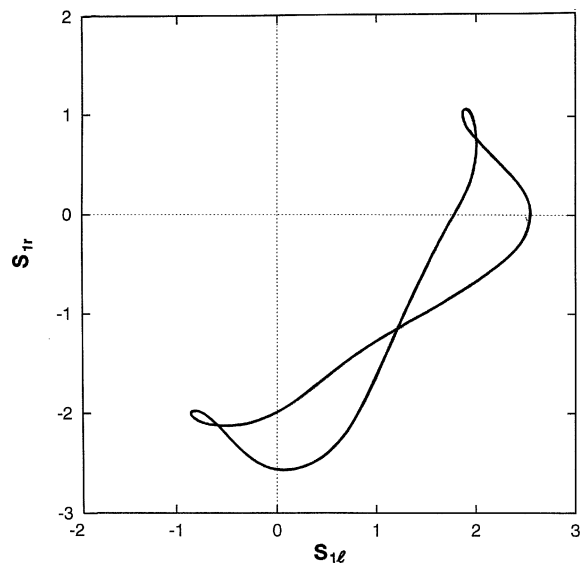

Figure 9. Phase trajectory of the oscillatory motion ($G = 45$; $G_Q = -30$).

As it is predicted by the linear theory, in a certain region in the plane (G, G_Q) the oscillatory motion appears in the system. For the oscillatory motions, the symmetry (20) is violated. For characterising the intensity and

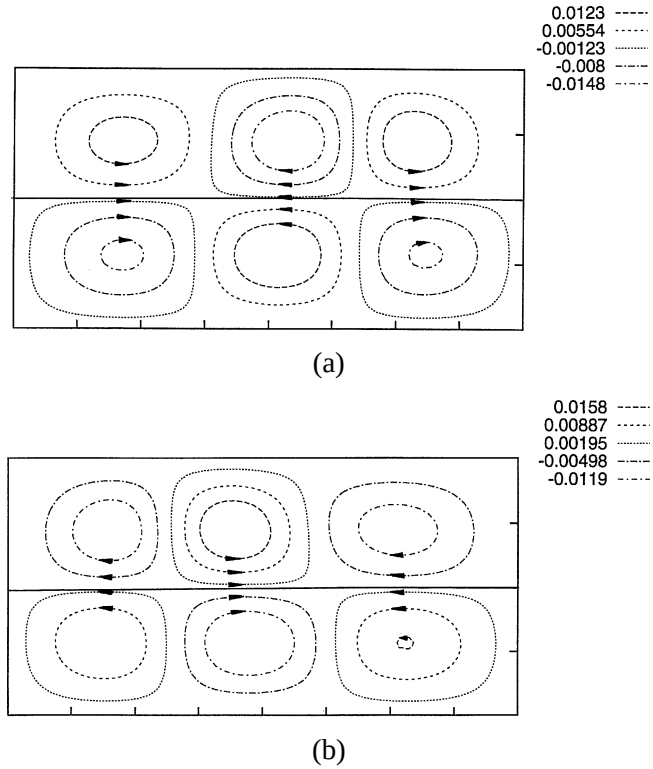

Figure 10. Streamlines for the oscillatory motion ($G = 45$; $G_Q = -30$).

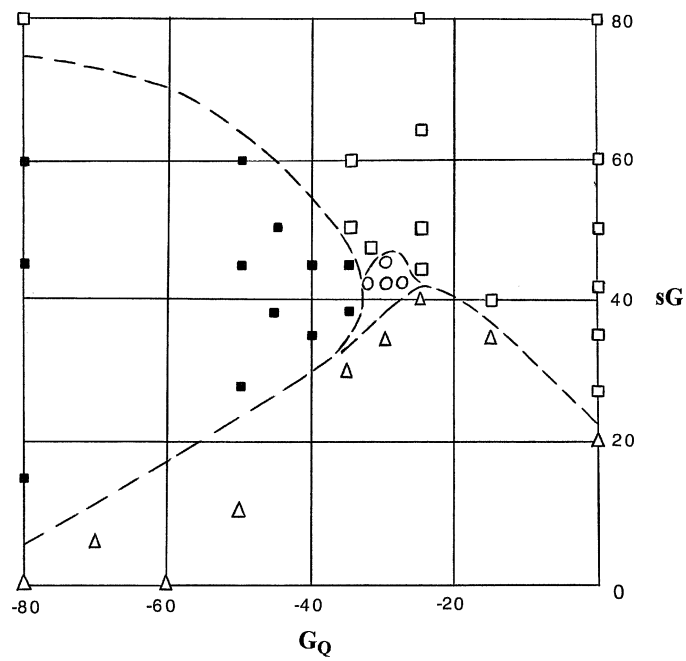

Figure 11. The diagram of regimes (△ – equilibrium, □ – steady state (type I), ■ – steady state (type II), ○ – oscillations). The dashed lines separate the regions of different regimes.

the structure of a non-symmetric convective flow, let us introduce the following integral variables:

$$S_{1l}(t) = \int_{-L/2}^{0} \mathrm{d}x \int_0^1 \mathrm{d}z \psi_1(x, z, t), \qquad S_{1r}(t) = \int_0^{L/2} \mathrm{d}x \int_0^1 \mathrm{d}z \psi_1(x, z, t).$$

The phase trajectory, which is constructed in the plane (S_{1l}, S_{1r}) is presented in *figure 9*. During one half of the period $\tau/2$ the corresponding vortices change their signs (see *figures 10*(a), (b)):

$$\psi_m(x, z, \tau/2) = -\psi_m(L - x, z, 0), \qquad T_m(x, z, \tau/2) = T_m(L - x, z, 0); \quad m = 1, 2.$$

The oscillatory motion exists only in (the small region of G and $|G_Q|$. With the increase in G or $|G_Q|$ a steady motion is realized in the system. The general diagram of regimes in the plane (G, G_Q) is shown *figure 11*.

5. Conclusion

The nonlinear regimes of anti-convection and Rayleigh–Benard convection in a system with heat release on the interface are considered. Anti-convective flow structures for the fluid system that have no anti-convection in the absence of heat sources (sinks) on the interface, were simulated. For Rayleigh–Benard convection the steady and oscillatory motions with different spatial structures were found. The region of oscillations is bounded by the regions of steady motions and the stability region of the mechanical equilibrium state.

Acknowledgements

This work was supported in part by the German–Israeli Foundation for Scientific Research and Development, the Israeli Science Foundation and by the Steigman Research Fund.

References

[1] Landau L.D., Lifshitz E.M., Fluid Mechanics, Pergamon Press, Oxford, 1987.
[2] Welander P., Convective instability in a two-layer fluid heated uniformly from above, Tellus 16 (1964) 349.
[3] Gershuni G.Z., Zhukhovitsky E.M., On the instability of a horizontal layer system of immiscible fluids when heating from above, Fluid Dyn. 15 (1980) 816.
[4] Simanovskii I.B., Convective stability of two-layer system, PhD thesis, Leningrad State University, 1980.
[5] Nepomnyashchy A.A., Simanovskii I.B., Onset of convection at heating from above and heat release on the interface, Izv. AN SSSR, Mekh. Zhidk. i Gaza 3 (1990) 16.
[6] Perestenko O.V., Ingel L.Kh., On a possible type of convective instability in the ocean-atmosphere system, Izv. AN SSSR Fiz. Atmosf. i Okeana 27 (1991) 408.
[7] Nepomnyashchy A.A., Simanovskii I.B., Braverman L.M., Anti-convection in systems with heat release on the interface, Phys. Fluids 12 (2000) 1129.
[8] Simanovskii I.B., Nepomnyashchy A.A., Convective Instabilities in Systems with Interface, Gordon and Breach, London, 1993.
[9] Kuskova T.V., Chudov L.A., On approximate boundary conditions for vortex at calculation of the flows of viscous incompressible fluid, Comput. Meth. Prog. 11 (1968) 27 (in Russian).
[10] Braverman L.M., Eckert K., Nepomnyashchy A.A., Simanovskii I.B., Thess A., Convection in two-layer systems with anomalous thermocapillary effect, Phys. Rev. E 62 (2000) 3619.
[11] Rao C.N.R., Chemical Applications of Infrared Spectroscopy, Academic Press, New York, 1963.